

Small- and large-scale distribution of microbes and biogeochemistry in the Great Barrier Reef

Catia Carreira ^{Corresp., 1}, Júlia Porto Silva Carvalho ², Samantha Duggan ², Isabel Pereira ³, Christian Lønborg ^{2,4}

¹ Departamento de Biologia & CESAM - The Centre for Environmental and Marine Studies, Universidade de Aveiro, Aveiro, Portugal

² Australian Institute of Marine Science, Townsville, Queensland, Australia

³ Departamento de Matemática & CIDMA - Center for Research and Development in Mathematics and Applications, Universidade de Aveiro, Aveiro, Portugal

⁴ Section for Applied Marine Ecology and Modelling, Department of Bioscience, Aarhus University, Roskilde, Denmark

Corresponding Author: Catia Carreira
Email address: ccd.carreira@gmail.com

Microbial communities distribute heterogeneously at small-scales (mm-cm) due to physical, chemical and biological processes. To understand microbial processes and functions it is necessary to appreciate microbes and matter at small scales, however, few studies have determined microbial, viral, and biogeochemical distribution over space and time at these scales. In this study, the small and large-scale spatial and temporal distribution of microbes (bacteria and chlorophyll *a*), viruses, dissolved inorganic nutrients and dissolved organic carbon were determined at five locations (spatial) along the Great Barrier Reef (Australia), and over 4 consecutive days (temporal) at a coastal location. Our results show that: 1) the parameters show high small-scale heterogeneity; 2) over the large scale the coastal location showed the highest average concentrations/abundances; 3) none of the parameters measured explained the bacterial distributions at these scales spatially or temporally; 4) chemical (ammonium, nitrate/nitrite, phosphate, dissolved organic carbon, and total dissolved nitrogen) and biological (chl *a*, bacteria, and viruses) measurements did not reveal significant relationships at the cm scale; and 5) differences were found between sites/days but without a clear pattern.

1 **Small- and large-scale distribution of microbes and biogeochemistry in the Great**
2 **Barrier Reef**

3

4 Cátia Carreira*¹, Júlia Porto Silva Carvalho², Samantha Duggan², Isabel Pereira³, Christian
5 Lønborg^{2,4}

6

7 ¹Departamento de Biologia & CESAM – Centro de Estudos do Ambiente e do Mar,
8 Universidade de Aveiro, Aveiro, Portugal

9 ²Australian Institute of Marine Science, Townsville, Queensland, Australia

10 ³Departamento de Matemática & CIDMA - Center for Research and Development in
11 Mathematics and Applications, University of Aveiro, Aveiro, Portugal

12 ⁴Section for Applied Marine Ecology and Modelling, Department of Bioscience, Aarhus
13 University, Denmark

14

15 *Corresponding author:

16 Cátia Carreira

17 Campus de Santiago, Aveiro, 3810-193, Portugal

18 Email address: ccd.carreira@gmail.com

19

20 **Abstract**

21 Microbial communities distribute heterogeneously at small-scales (mm-cm) due to physical,
22 chemical and biological processes. To understand microbial processes and functions it is
23 necessary to appreciate microbes and matter at small scales, however, few studies have
24 determined microbial, viral, and biogeochemical distribution over space and time at these
25 scales. In this study, the small and large-scale spatial and temporal distribution of microbes

26 (bacteria and chlorophyll *a*), viruses, dissolved inorganic nutrients and dissolved organic
27 carbon were determined at five locations (spatial) along the Great Barrier Reef (Australia),
28 and over 4 consecutive days (temporal) at a coastal location. Our results show that: 1) the
29 parameters show high small-scale heterogeneity; 2) over the large scale the coastal location
30 showed the highest average concentrations/abundances; 3) none of the parameters measured
31 explained the bacterial distributions at these scales spatially or temporally; 4) chemical
32 (ammonium, nitrate/nitrite, phosphate, dissolved organic carbon, and total dissolved nitrogen)
33 and biological (chl *a*, bacteria, and viruses) measurements did not reveal significant
34 relationships at the cm scale; and 5) differences were found between sites/days but without a
35 clear pattern.

36

37 **Introduction**

38 Marine bacterioplankton and phytoplankton and their associated functions are the primary
39 controls of energy and material cycling in the global ocean. How they interact with the
40 environment is therefore of pivotal importance for understanding ocean food web structure
41 and biogeochemical processes (Wiens, 1989). Depending on the process to be studied, the
42 scale of spatial resolution has to be adjusted accordingly. As microbes interact at the cellular
43 level, it is essential to describe microbial community ecology at small scales (mm to cm) to
44 capture the microbial functions and productivity in marine environments (Azam and Malfatti,
45 2007). There is evidence that microbes distribute heterogeneously at small scales in marine
46 environments (Azam and Long, 2001), which has been linked to biological factors (e.g.,
47 grazing, lysis), and interactions between microbes and the environment (e.g., organic matter,
48 aggregates) (e.g., Seymour et al., 2006; Stocker et al., 2008). Viruses are estimated to kill
49 between 20-40% of the prokaryotic community every day, with major consequences for the
50 microbial diversity and carbon cycling (Suttle, 2005). However virus-microbes's relationship

51 is not always straightforward. Viruses are typically tightly coupled with bacterial
52 communities when large datasets are used (Wigington et al., 2016), however when small
53 datasets or small volumes are used, bacteria and viruses are not coupled (Bouvy et al.,
54 2012;Carreira et al., 2013). This difference is probably a result of the time lag between
55 infection and replication which is easier to observe at smaller scales and volumes (Carreira et
56 al., 2013). It has also been demonstrated that prokaryotes can move towards a chemical cue
57 (chemotactic behaviour), as a response to point sources of organic and inorganic matter
58 (Malmcrona-Friberg et al., 1990;Hütz A, 2011). This chemotactic behaviour has been
59 suggested to increase the microbial degradation of dissolved organic matter (DOM) (Fenchel,
60 2002), and heterogeneous environments are suggested to have higher phytoplankton
61 production than found under homogeneous condition (Brentnall et al., 2003). Such findings
62 have implications for the way we frame marine biogeochemical cycling by microbes. Models
63 have been used previously to understand the interaction between microbes and organic matter
64 at small scales (e.g., Datta et al., 2015), while other studies have used controlled experiments
65 (e.g., Brumley et al., 2019), and measured microbial distribution at small scales in a natural
66 ecosystem (e.g., Seymour et al. 2005). But none of these have measured the chemical (organic
67 and inorganic) components interacting with the microbes at small scales in a natural
68 ecosystem.

69 The Great Barrier Reef (GBR) is situated on the continental shelf and slope of
70 Australia's north-eastern coast and is the largest contiguous coral reef system in the world.
71 The GBR has a total of ~ 3700 reefs which are mainly located away from shore; with the
72 open water body separating the reef matrix from the mainland known as the GBR lagoon. The
73 system is characterized by stable high temperatures, oligotrophic, sunlit, and alkaline waters
74 (Furnas et al., 2011;Uthicke et al., 2014). The microbial patchiness at the cm scale has been
75 studied by Seymour et al. (2005) on one reef, demonstrating a 2- to 3.5-fold changes in the

76 viral and bacterial concentrations over a distance of 12 cm above coral colonies. This
77 microbial heterogeneity suggests that small-scale interactions could be important in
78 understanding the microbial ecology and biogeochemistry of this system. But it remains to be
79 understood how representative these single measurements are for other locations in the GBR
80 and how this might vary over temporal scales.

81 In this study we determined the spatial and temporal variability in the small-scale
82 distribution of microbes (bacteria, and chlorophyll *a* – a proxy for phytoplankton biomass),
83 and viruses, as well as biogeochemical variables (dissolved inorganic nutrients and dissolved
84 organic carbon) at five locations along the GBR, and over 4 consecutive days at a coastal
85 location.

86

87 **Material and methods**

88

89 **Study sites and sampling**

90 Samples were collected at six sites spanning from coast to the outer reef in the Great
91 Barrier Reef (GBR; Fig 1; Table 1). Sites 1, 2, 3, and 5 were at coral reefs, site 4 was in the
92 Coral Sea, and site 6 was at the Australian Institute of Marine Science (AIMS) harbour
93 (Bowling Green Bay; Fig 1). Site 4 (Coral Sea) was used as a reference non-coral site. Site 6
94 (Bowling Green Bay) is located in the inner zone of the GBR, has no coral coverage and is
95 dominated by a nearby saltmarsh and small river. All coral reef sites showed clumps of
96 floating *Trichodesmium* spp. at the surface (Carreira pers. observ.) at the time of sampling. To
97 determine the spatial variability in the small-scale distribution of microbes, viruses and
98 biogeochemical measurements, surface water samples were collected once at sites 1 to 5 (Fig
99 1, Table 1; 17 to 22 December 2014). The temporal variability in the small-scale distribution
100 was determined at site 6 with samples collected during high tide every 24h over four

101 consecutive days (Fig 1, Table 1; 12 to 15 January 2015). Although 24h is not a temporal
102 small scale, the objective was only to understand the changes in spatial small scale over time.
103 Niskin bottle samples collected at site 6, at the same time and days as the temporal study
104 (days 1 to 4), were used as controls for the standard sampling method.

105 Samples were collected with a purpose built device consisting of 25 inlets (5 x 5) (Fig
106 2). With the help of a lever, all samples were collected manually, at the same time from 0.5 m
107 below the sea surface with the sampling taking about 5 seconds. As our objective was to
108 understand small-scale heterogeneity in the coral reef system, samples from sites 1, 2, 3, and
109 5 were taken above the coral reefs, but not in the proximity of a coral as done by Seymour et
110 al. (2005). Each inlet was connected to a 25 mL syringe each separated by 7 cm, representing
111 a total sampling area of 784 cm². This distance between the syringes was calculated to
112 account for the volume necessary for all measurements (25 mL) without interfering with
113 neighbouring sampling volumes. In this calculation we assume that the rapid intake of water
114 by the syringes is similar in shape to a turbulent jet (Pope, 2000). The following equations
115 were used for the calculation:

116

$$117 \quad V = \pi \times r^2 \times \frac{h}{3} \quad (1)$$

$$118 \quad \tan \theta = \frac{r}{h} \quad (2)$$

$$119 \quad r = \left(\frac{3 \times V \times \tan \theta}{\pi} \right)^{\frac{1}{3}} \quad (3)$$

120

121 we combined equations 1 and 2 to obtain the minimum distance (r) between syringes
122 (equation 3, Fig S1). Equation (1) calculates the volume of a cone (V), which is the water
123 rapidly sucked up ('turbulent jet') by the syringe and equation (2) takes into account its shape.
124 This allowed to calculate the distance (r) using a known angle of 11.8° (equation (3); Fig S1)

125 (Pope, 2000;Cushman-Roisin, 2019). This angle is always the same independent of the fluid
126 used (Cushman-Roisin, 2019).

127 At sites 1 to 5 temperature and salinity were recorded using a conductivity-
128 temperature-depth (CTD) profiles (Seabird SBE19Plus). At site 6 salinity samples were
129 collected and analysed in the laboratory with a Portasal Model 8410A, while temperature was
130 measured manually. Salinity and temperature varied between 32.0 and 35.6, and 28.7 and 32.0
131 °C, respectively (Table 1). From each syringe samples were collected for dissolved inorganic
132 nutrients (ammonium - NH_4^+ , nitrate/nitrite - $\text{NO}_3^-/\text{NO}_2^-$, and phosphate - HPO_4^{2-}), dissolved
133 organic carbon (DOC), total dissolved nitrogen (TDN), chlorophyll *a* (chl *a*), and bacterial
134 and viral counts. A precombusted (450°C, 4 h) GF/F filter (13 mm diameter) was used to
135 filter 5 mL for inorganic nutrients analysis, and 10 mL of seawater for DOC and TDN
136 analysis. DOC and TDN samples were fixed with 50 µL of 25 % H_2PO_4 and kept at 4 °C,
137 whereas inorganic nutrients were filtered and kept at -20 °C until analysed. The GF/F filters
138 used for collecting inorganic nutrients, DOC, and TDN samples were snap-frozen in liquid
139 nitrogen and kept at -20 °C for chl *a* extraction. All syringes, filter-holders and inorganic
140 nutrient sample tubes were acid-washed in 10 % HCl for 24 h, and then washed three times
141 with Milli-Q water before use.

142 For bacterial and viral counts, unfiltered subsamples of 1 mL, were collected in sterile
143 2 mL Eppendorf tubes and fixed with 0.5 % glutaraldehyde final concentration (25 % EM-
144 grade, Merck) for 15 min at 4 °C, after which samples were snap-frozen in liquid nitrogen and
145 stored at -80 °C until analysis by flow cytometry (FCM).

146

147 **Samples analysis**

148 Inorganic nutrients (NH_4^+ , $\text{NO}_3^-/\text{NO}_2^-$ and HPO_4^{2-}) were determined by standard
149 segmented flow analysis (SFA) as described in Hansen & Koroleff (1999). As all the

150 determined NH_4^+ concentrations were below the detection limit of the method ($<0.02 \mu\text{mol L}^{-1}$
151 ¹⁾ the data is not shown. The detection limit and precisions for the other parameters were:
152 $0.02 \mu\text{mol L}^{-1}$ for $\text{NO}_3^-/\text{NO}_2^-$ and $0.001 \mu\text{mol L}^{-1}$ for HPO_4^{2-} . Please note that the HPO_4^{2-}
153 concentrations at site 2 were also below the detection limit and therefore the data is not
154 shown. DOC and TDN concentrations were measured using a Shimadzu TOC-L carbon
155 analyser coupled in series with a nitric oxide chemiluminescence detector according to
156 Lønborg et al. (2018). Three to five replicate injections of $150 \mu\text{L}$ were performed per sample.
157 Concentrations were determined by subtracting a Milli-Q blank and dividing by the slope of a
158 daily standard curve of potassium hydrogen phthalate and glycine. Using the deep ocean
159 reference (Sargasso Sea deep water, 2600 m) we obtained a concentration of $45.6 \pm 1.8 \mu\text{mol}$
160 L^{-1} (average \pm SD) for DOC and $22.0 \pm 1.5 \mu\text{mol L}^{-1}$ for TDN. Please note that the TDN
161 measurements for day 2 and 3 of the temporal study are not reported due to problems with the
162 gas supply for the nitric oxide chemiluminescence detector during these specific sample runs.
163 The detection limit for DOC and TDN were $8 \mu\text{mol L}^{-1}$ and $0.02 \mu\text{mol L}^{-1}$, and the precisions
164 were $\pm 1 \mu\text{mol L}^{-1}$ and $\pm 0.3 \mu\text{mol L}^{-1}$, respectively.

165 Chl *a* determinations were made by extracting the GF/F filters in ethanol (96 %) for 8
166 h. Samples were analysed spectrophotometrically according to Strickland & Parsons (1972).
167 The detection limit and precision for the chl *a* method were $0.005 \mu\text{g L}^{-1}$ and $\pm 0.05 \mu\text{g L}^{-1}$,
168 respectively. Flow cytometric (FCM) enumeration of bacteria and viruses was carried out
169 using a standard bench top Becton-Dickinson FACSVerse FCM, equipped with an air-cooled
170 argon laser (excitation 488 nm, 15 mW power) according to Gasol et al. (1999) and Brussaard
171 (2004) for bacteria and viruses, respectively. Samples were diluted (5-60 times) in TE buffer
172 (Tris 10 mM, EDTA 1 mM, pH 8.0), stained with SYBR Green I (Molecular Probes[®],
173 Invitrogen Inc., Life Technologies[™], NY, USA) to a final concentration of 10^{-4} of the
174 commercial stock solution. Bacterial samples were incubated at ambient temperature, whereas

175 viral samples were incubated at 80 °C (Brussaard, 2004), both in the dark for 10 min. The
176 trigger was set for green fluorescence and the data was analysed using Flowing Software
177 2.5.1. (freeware; <http://flowingsoftware.btk.fi>). The event rate was 300 bacteria s⁻¹ and
178 between 300-800 viruses s⁻¹ to avoid coincidence (Gasol et al., 1999;Brussaard, 2004). We
179 would like to note that recent research (e.g., (Forterre et al., 2013) has suggested that viral
180 counts might also include gene transfer agents (GTAs), membrane -derived vesicles (MVs),
181 or even cell debris that might be confused with viruses. However currently there is no method
182 to distinguish between all these particles, therefore, we assumed that the viral counts made by
183 FCM are viruses.

184 Inorganic nutrients, DOC, TDN, and chl *a* concentration, and bacterial and viral
185 abundances data were plotted using Surfer 9.0.

186

187 **Statistical analyses**

188 To measure small-scale heterogeneity within each site/day it was used the coefficient
189 of variation (CV) calculated as the (Standard deviation/Mean) × 100.

190 To understand differences in concentrations/abundance between sites/days, boxplots
191 were made using the average values for each site/day. To compare the distributions of the
192 independent samples, the non-parametric Kruskal-Wallis tests were performed for the spatial
193 and temporal data sets because for each variable at least one subgroup (for site or day) failed
194 the normality condition for parametric tests (Agresti, 2007), i.e., the values of each variable
195 did significantly change over the locations. Multiple comparison tests were also performed to
196 understand which pairs of sites/days had the biggest differences. For these pairwise
197 comparisons two tests were performed: Nemenyi tests with Chi-squared approximation and
198 the Dunn's tests for multiple comparisons with the Bonferroni adjustment method (Dun,
199 1964).

200 To identify which variables were more linearly correlated, and determine the
201 correspondent magnitude, Pearson correlation coefficient were calculated, considering each
202 site and all sites combined as well as each day and all days combined.

203 To understand the relation between the parameters, independent of the site and day,
204 factor analysis was applied to the data. A factor analysis is used to describe an eventual
205 correlation between several observed variables in regard to another group of non-observed
206 variables, of smaller dimension, named factors (Johnson and Wichern, 2007). To perform the
207 factor analysis all variables were considered, regardless of site, as there were no significant
208 correlations between the variables, according to Bartlett's test of sphericity (p value < 0.001).
209 In order to classify the variables cluster analyses were performed in the spatial and temporal
210 data. For the temporal data cluster analysis was tested, but without meaningful results. For
211 the statistical analyses R (1.1.442) and SPSS (v25) software were used.

212

213 **Results**

214

215 **Small scale variability**

216 Using the coefficient of variability (CV) as a measure of heterogeneity, generally, in
217 the spatial and temporal studies, there was a high small-scale heterogeneity (up to 76 % for
218 chl *a*) for chl *a*, $\text{NO}_3^-/\text{NO}_2^-$ and HPO_4^{2-} and lower heterogeneity for DOC, bacteria and
219 viruses. With the exception of chl *a*, the chemical variables were more variable, than the
220 biological within each site and day (Table 2 and 3). Next is given a description of the small-
221 scale variability for each parameters for the sites and days measured.

222 In the spatial study of $\text{NO}_3^-/\text{NO}_2^-$, site 5 showed the lowest heterogeneity (10 %),
223 while site 1 had the highest (37 %; Table 2, Fig. 3). In the temporal study, the highest
224 variability was observed at day 1 (45 %) and lowest at day 3 (10 %) (Table 3, Fig 5).

225 Maximum differences observed between two nearby points in the spatial and temporal studies
226 were of 2.6 x and 3.6 x, respectively (Fig 3 and 5). Also site 1 showed the highest
227 heterogeneity in HPO_4^{2-} concentrations (27 %), and sites 4 and 5 the lowest (20%; Table 2,
228 Fig 3). In the temporal study the heterogeneity was highest at day 4 (26 %), and lowest at day
229 3 (10 %; Table 3, Fig 5). The maximum variability between nearby points was of 2.4 x, both
230 spatially and temporally. DOC concentrations showed the highest heterogeneity at sites 2 and
231 3 (13 %; Table 2, Fig 3), while the lowest was found at site 5 (6 %). DOC showed the lowest
232 heterogeneity of all measured parameters at all sites. The DOC concentrations in the temporal
233 study were higher than in the spatial study, but the heterogeneity was lower. The highest
234 heterogeneity was of 5 % at day 3, and the lowest just 4 % all other days (Table 3, Fig 5). A
235 maximum variability of 1.5 x and 1.2 x between two nearby point was found spatially and
236 temporally. Finally, TDN varied most at site 3 (24 %) and least at site 4 (9 %; Table 2, Fig 3).
237 A maximum variability of 3 x was found between points. In the temporal study, TDN was
238 only measured on days 1 and 4, and the heterogeneity was low in those two days measured (9
239 and 6 %).

240 Chl *a* showed the highest variability of all parameters, with the highest heterogeneity
241 at site 5 (68 %) and the lowest at site 2 (43 %; Table 3, Fig 6). In the temporal study the
242 heterogeneity was higher than found in the spatial study, with a maximum at day 3 (76 %).
243 Differences between nearby points were 7.9 x and 25.5 x, spatially and temporally.

244 Bacterial and viral abundances showed generally similar and low heterogeneity both
245 spatially and temporally, with viral abundances being nearly 1 order of magnitude higher than
246 bacteria. Bacterial abundances showed similarly low heterogeneity at site 2 and day 1 (4 %
247 and 5 %), and high at site 3 and day 3 (15 % and 19 %; Table 2 and 3, Fig 4 and 6). Viral
248 abundances showed lowest heterogeneity at sites 1 and day 1 (6 % and 9 %), while highest
249 heterogeneity was found at sites 2 and 3, and day 2 (15 % and 13 %; Table 2 and 3, Fig 4 and

250 6). Finally, the VBR showed low heterogeneity at sites 4 and 5 (9 %) and day 1 (10 %), and
251 highest heterogeneity was observed at site 3 (15 %) and day 3 (20 %; Table 2 and 3, Fig 4 and
252 6).

253 Overall, although no clear pattern emerged, site 3 (furthest north) and day 3 (high
254 nutrient concentrations) had most parameters with highest heterogeneity, while site 5 (furthest
255 south) and day 1 (low nutrient concentrations) had most parameters with the lowest
256 heterogeneity.

257

258 **Large scale variability**

259 All sites showed comparable concentrations/abundances overall, with the exception of
260 bacterial and viral abundances at the non-coral site 4 (Coral Sea) that were on average 1.8 x
261 and 2.6 x lower compared to the other sites (Table 2, Fig 4). Over the four days, nutrient
262 concentrations increased while bacterial and viral abundances decreased, and chl *a* and VBR
263 showed no differences (Table 3, Fig 6, Fig S2). The inorganic nutrients ($\text{NO}_3^-/\text{NO}_2^-$ and
264 HPO_4^{2-}) showed comparable average concentrations between the outer reef and Coral Sea
265 sites (Table 2, Fig 3), and to site 6 (temporal study; Table 3; Fig 5), except for day 4 when
266 concentrations increased by 11.0 x and 1.4 x compared to day 1 (lowest concentrations, but
267 still comparable to the sites). DOC was slightly higher at site 6 (average range over the 4
268 days: $100 \pm 4 \mu\text{mol L}^{-1}$ to $118 \pm 6 \mu\text{mol L}^{-1}$; Table 3, Fig 5), compared to the coral sites
269 (average range over sites 1, 2, 3, and 5: $83 \pm 11 \mu\text{mol L}^{-1}$ to $90 \pm 9 \mu\text{mol L}^{-1}$) and Coral Sea
270 site ($89 \pm 8 \mu\text{mol L}^{-1}$; Table 2, Fig 3). TDN showed slightly higher concentrations at site 6
271 (particularly day 4) compared to the other sites (Table 2 and 3, Fig 3 and 5). Chl *a* was on
272 average lower at site 6 compared to all other sites (Table 2 and 3, Fig 4 and 6). Bacterial and
273 viral abundances were on average higher at site 6 (total average of the 4 days: $18.1 \pm 3.1 \times 10^5$
274 mL^{-1} and $104.8 \pm 17.3 \times 10^5 \text{ mL}^{-1}$, respectively; Table 3, Fig 6), compared to the coral sites

275 (average range: $7.8 \pm 0.5 \times 10^5 \text{ mL}^{-1}$ to $12.5 \pm 1.9 \times 10^5 \text{ mL}^{-1}$; and $41.3 \pm 2.7 \times 10^5 \text{ mL}^{-1}$ to
276 $58.2 \pm 8.8 \times 10^5 \text{ mL}^{-1}$ respectively; Table 2, Fig 4). Overall site 6 (temporal study) showed
277 either similar or slightly higher concentrations/abundances when compared to the other sites
278 (coral sites and non-coral - Coral Sea), but these results should be taken with cautions as there
279 was no temporal follow-up at sites 1 to 5.

280 Comparing the concentrations and abundances obtained with a Niskin bottles during
281 the temporal study (Table S5) with the range of values for each parameter over the 4 days
282 (Table 3), the values are generally within these ranges, hence also showing the increase in
283 nutrients and decrease in bacterial and viral abundances over the 4 days.

284 For each variable ($\text{NO}_3^-/\text{NO}_2^-$, HPO_4^{2-} DOC, Chl *a*, TDN, bacteria, viruses) pairwise
285 comparisons between sites and days were performed. The Kolmogorov-Smirnov tests showed
286 that the spatial and temporal data are not normally distributed for each variable. Concerning
287 each variable in the study, the Kruskal-Wallis test revealed that at least one of the samples for
288 each site/day is significantly different from the others. However, the pairwise comparisons
289 using suitable non-parametric tests for multiple comparisons (Nemenyi-tests with Chi-squared
290 approximation and Dunn's tests) did not point to a common pattern, nonetheless the p values
291 are shown in the supplement material (Table S3 and S4). Overall, statistically significant
292 differences were found, but there were no clear patterns spatially or temporally as determined
293 by non-parametric tests, i.e., no site and day or combinations of sites and days showed a trend
294 or similar behaviour for all the parameters or a subsection of these (Fig 7 and 8). DOC
295 showed the least statistical differences between sites (Fig 7, Table S3), while chl *a* showed the
296 least differences between days (Fig 8, Table S4).

297 Correlations were determined between all parameters within a site/day and between
298 sites/days without any clear results (Table S1 and S2). Most correlations did not exhibit a
299 strong linear relationship between the variables in study (Table S1 and S2). However it can be

300 highlighted that spatially, bacteria correlated negatively with HPO_4^{2-} and viruses ($n = 25$, $R^2 =$
301 -0.54 and 0.55 , respectively) and temporally bacteria correlated negatively with $\text{NO}_3^-/\text{NO}_2^-$
302 and HPO_4^{2-} ($n = 25$, $R^2 = -0.75$ and -0.50). The correlation between all bacterial and all viral
303 abundances (spatial and temporal) showed a positive correlation ($n = 325$, $R^2 = 0.75$; Fig 9).
304 This correlation showed an intercept not significantly different from zero, indicating a tight
305 link between viruses and bacteria.

306 Although no relations were found between the parameters at the different sites and
307 days, factor analysis was applied to understand the relation between the parameters. The
308 factor analysis showed that the variables can be decomposed into two factors, the chemical
309 ($\text{NO}_3^-/\text{NO}_2^-$ and DOC) and biological (bacteria, chl *a* and viruses) groups (Fig. S3). It should
310 be noted that HPO_4^{2-} and TDN were excluded from this analysis because the correspondent
311 anti-image matrices values were smaller than 0.5 (0.340 and 0.372, respectively) meaning that
312 we are discarding these variables since its partial correlation values are considered too small
313 to apply factorial analysis. Overall these results show: 1) that the chemical variables (NO_3^-
314 $/\text{NO}_2^-$ and DOC) are more related to each others than to the biological variables (bacteria, chl
315 *a* and viruses), and likewise for the biological variables, 2) the chemical variables do not
316 explain the bacterial distribution, and 3) given the biological variables are more related to
317 each others, there is a higher likelihood they could explain the bacterial distribution, but the
318 results are insufficient to make a firm conclusion. Cluster analysis showed (Fig. S4A) a clear
319 grouping between the biological (bacteria, viruses and chl *a*) and the chemical ($\text{NO}_3^-/\text{NO}_2^-$,
320 HPO_4^{2-} , DOC and TDN) between all sites, whereas the classification was less clear between
321 the days (Fig. S4B). Here bacteria and viruses grouped together, while DOC, chl *a*, NO_3^-
322 $/\text{NO}_2^-$ and HPO_4^{2-}) clustered. Please note that the TDN data was not included in this analysis
323 as there was no data for days 2 and 3. These results suggest that the measured scales (cm) are

324 most probably not appropriate to understand the relation between nutrients (organic and
325 inorganic), and the microbial and viral communities.

326

327 **Discussion**

328 A major challenge in microbial ecology is to understand how microbial communities
329 are influenced by changing environmental conditions. To date, however, most studies have
330 explored these links using both larger volumes (litres) and spatial scales (km), ignoring that
331 the water column is in fact heterogeneous at smaller scales (Azam and Malfatti, 2007).
332 Previous theoretical and laboratory based studies have suggested that both microbes and their
333 growth substrates (DOC, inorganic nutrients) have a variable distribution at small scale
334 (Blackburn et al., 1998; Blackburn and Fenchel, 1999), but few studies have actually
335 determined this combined heterogeneity in field studies (Seymour et al., 2006). Our study
336 shows the first *in-situ* heterogeneous 2-dimensional distribution of chemical (ammonium,
337 nitrate/nitrite, phosphate, dissolved organic carbon, and total dissolved nitrogen) and
338 biological (chl *a*, bacteria, and viruses) variables at the cm scale over spatial and temporal
339 scales. Nonetheless the authors are aware that the small scale of observation used in this study
340 (cm) does not fully replicate the differences in scale of interactions between the
341 biogeochemistry and microbes. However this study is intended as a first approach to
342 understand these interactions and more detailed studies at smaller scales are therefore needed.
343 Furthermore, we have used this large dataset with 25 replicates per site/day to compare the
344 data between sites and days.

345 At the resolution of our measurements none of the variables ($\text{NO}_3^-/\text{NO}_2^-$, HPO_4^{2-} ,
346 DOC, TDN, chl *a*, or viruses) explained the small-scale distribution of bacteria at the studied
347 sites and days (Table S1 and S2). Nonetheless site 3 (furthest north) showed more parameters
348 with higher heterogeneity, compared to site 5 (furthest south). At site 6 (Bowling Green Bay),

349 day 3 showed more parameters with higher heterogeneity compared to day 1. The increase of
350 nutrients in Bowling Green Bay, observed at day 3, could explain the higher heterogeneity
351 observed at this day, perhaps as a results of chemotactic behaviour by the microbes in search
352 of food (Malmcrona-Friberg et al., 1990;Hütz A, 2011).

353 The high variability of chl *a* (indicative of phytoplankton biomass) and nutrients found
354 in both the spatial and temporal studies could be caused by distinct heterogeneous
355 microenvironments created by ‘Phycosphere’ patches (nutrient rich areas surrounding
356 phytoplankton cells resultant from their excretion), suggested to be hotspots for bacterial
357 growth (Stocker and Seymour, 2012). However, bacterial growth was not measured in our
358 work, and no clear link between chl *a* or nutrients and bacterial abundances was observed at
359 the scale sampled. Additionally, the low variability observed for bacteria, viruses and DOC
360 might suggest that the sample sizes collected for analysis (1 and 10 mL) is too large to
361 determine heterogeneity, but it could also be due to that most DOC is refractory and large
362 proportions of cells may be dormant (Giorgio and Scarborough, 1995;Lønborg et al., 2018).
363 Furthermore, the distribution of biological and chemical variables in the ocean are known to
364 be impacted by processes occurring at a range of scales; for example, at the centimetre scale
365 marine snow formation is important, while at kilometre scales fronts and eddies can shape the
366 distribution of both chemical and biological variables (Kjørboe, 2001;Jickells et al.,
367 2008;Baltar and Aristegui, 2017).

368 The concentrations of the chemical parameters and chl *a* were comparable to previous
369 studies in the GBR (Furnas et al., 2005;Lønborg et al., 2018). Viral and bacterial abundances
370 found in our study were within the estimates found for middle shelf reef surface waters in the
371 GBR (Alongi et al., 2015), but about 4 - 6 and 5 - 7 x higher than those determined from a
372 coastal coral reef in the GBR (Seymour et al., 2005), respectively. The Niskin bottle samples
373 taken at site 6 (temporal study) also showed concentrations and abundances within the ranges

374 of the small-scale sampling. However, sampling using a Niskin bottle clearly misses the high
375 small-scale heterogeneity determined using the cm scale device from the present study.
376 Overall, the average concentrations from the temporal study were higher than in the spatial
377 study, which was expected as the temporal station was closer to shore.

378 On the whole, no pattern could be statistically detected, suggesting that the controlling
379 factors and dynamics were different between sites and days. Some variability in the spatial
380 study could be attributed to the differences in sampling time as our temporal study also
381 showed differences. However the differences observed between days (Table 3; Fig S2) are
382 comparable to the differences observed between sites (Table 2), suggesting that differences
383 between sites cannot solely be due to different sampling times. In the temporal study
384 differences in the variability became more obvious over time, with nutrient concentrations
385 increasing, while bacteria and viruses showed an overall decrease in abundances. Previous
386 studies have also suggested that the heterogeneous distribution of microbes could be linked
387 with chemical (e.g., substrate), physical (e.g., turbulence) and/or biological (e.g., viral lysis)
388 processes or a combination of these (Stocker et al., 2008; Durham et al., 2013; Carreira et al.,
389 2015). A likely explanation for the spatial differences could be the variability in the quality
390 and type of substrate, with one previous study showing spatial differences (km scale) in the
391 concentrations of potential microbial substrate (i.e., carbohydrates and proteins) in the GBR
392 (Lønborg et al., 2017). Another important factor to consider for both the spatial and temporal
393 variability is turbulence, which increases the heterogeneity of swimming phytoplankton by
394 10-fold (Durham et al., 2013). Other studies have found spatial differences in the composition
395 of the microbial communities (both phytoplankton and bacteria) in the GBR, which could
396 have impacted the results in our spatial component (Revelante et al., 1982; Angly et al., 2016).
397 Grazing by microzooplankton could also have influenced the spatial and temporal variability,
398 particularly of phytoplankton, as shown by the high mortality rates (75%) by

399 microzooplankton of phytoplankton in tropical/subtropical regions (Calbet and Landry 2004).
400 Cell lysis might also have impacted the distributions of phytoplankton and bacteria, but we
401 currently lack sufficient data to conclude if this is a cause for the variability found in this
402 study. Specifically, for the temporal study, which took place at an inshore station, the daily
403 differences in nutrient level could also have been caused by variable inputs from the nearby
404 river and/or sediment resuspension, which both have been shown to increase nutrients
405 concentrations in inshore parts of the GBR (Lambrechts et al., 2010).

406 The negative correlations found between nutrients ($\text{NO}_3^-/\text{NO}_2^-$ and HPO_4^{2-}) and
407 bacteria could be explained by a discrepancy between the timescales of nutrient uptake and
408 bacterial growth, or bacterial growth could be limited by other factors than N and P (e.g.,
409 carbon, iron) and they therefore did not take up these nutrients (Pinhassi et al., 2006). No
410 correlations were found between bacterial and viral abundances for individual sites or days (n
411 = 25), but when combining all data, a relationship was observed ($n = 325$, $R^2 = 0.75$; Fig. 9).
412 A lack of relationship between viruses and bacteria has previously been found in another
413 study in a reef system with a small sample size ($n = 36$) (Bouvy et al., 2012), suggesting that
414 small datasets might capture mismatched communities. This effect is then averaged out when
415 larger datasets are pulled together (Wigington et al., 2016). Likewise the lack of relations
416 between bacteria and organic and inorganic nutrients could result from a discrepancy between
417 assimilation and observable changes. Thus, as most oceanographic studies collect larger
418 samples (e.g., litres) or areas (e.g., kilometres) the interactions between microbes and viruses
419 at small scales will not be included. Likewise, we also show that “similar” sites (reef sites)
420 show a high degree of heterogeneity between them. Our results therefore indicate that caution
421 is necessary when using one site or time point as a reference and it is important to consider
422 the scale of observation to obtain an accurate understanding of microbial interactions.

423 In conclusion the spatial study showed: 1) high small-scale variability across coral and
424 non-coral sites; 2) lower bacterial and viral abundances in the Coral Sea compared to coral
425 sites, and 3) the Northern most site had more heterogeneous parameters than the southernmost
426 site. The temporal study showed: 1) persistent high small-scale heterogeneity over time, 2)
427 24h is not an appropriate measure of temporal change, instead, shorter time periods should be
428 used, 3) day 3, with higher nutrient concentration, also showed more heterogeneous
429 parameters, compared to day 1 with lower nutrients concentrations, 4) Niskin bottle samples
430 showed a similar variability, but missed the heterogeneity observed using the device
431 presented, and 5) variability observed across days is comparable to that across sites, hence
432 differences between sites cannot only be attributed to different sampling times.

433 Overall, this study shows that at the cm scale measured in the GBR: 1) parameters
434 show high small-scale heterogeneity, 2) over the large scale the coastal location showed the
435 highest average concentrations/abundances; 3) none of the parameters could explain the
436 small- or large- scale distribution of bacteria spatially or temporally; 4) at the scales
437 measured no significant relation were found, and 5) statistical differences were found for the
438 measured parameters between sites and days.

439

440 **Acknowledgements**

441 We thank the crew of the R.V. Cape Ferguson for help at sea. The help of the Cruise leader
442 (Sven Uthicke) and participant is also acknowledged. We are thankful to Niall Jeeves for
443 building the microsampling device and Jessica Benthuisen for the calculation of the required
444 minimal distance between samples.

445

446

447 **References**

- 448 Agresti, A. (2007). *An Introduction to Categorical Analysis*. Wiley.
- 449 Alongi, D.M., Patten, N.L., Mckinnon, D., Köstner, N., Bourne, D.G., and Brinkman, R.
450 (2015). Phytoplankton, bacterioplankton and virioplankton structure and function
451 across the southern Great Barrier Reef shelf. *Journal of Marine Systems* 142, 25-39.
- 452 Angly, F.E., Heath, C., Morgan, T.C., Tonin, H., Rich, V., Schaffelke, B., Bourne, D.G., and
453 Tyson, G.W. (2016). Marine microbial communities of the Great Barrier Reef lagoon
454 are influenced by riverine floodwaters and seasonal weather events. *PeerJ* 4, e1511.
- 455 Azam, F., and Long, R.A. (2001). Sea snow microcosms. *Nature* 414, 495-498.
- 456 Azam, F., and Malfatti, F. (2007). Microbial structuring of marine ecosystems. *Nature*
457 *Reviews: Microbiology* 5, 782-791.
- 458 Baltar, F., and Aristegui, J. (2017). Fronts at the surface ocean can shape distinct regions of
459 microbial activity and community assemblages down to the bathypelagic zone: the
460 Azores front as a case study. *Frontiers in Marine Science* 4, 252.
- 461 Blackburn, N., and Fenchel, T. (1999). Influence of bacteria, diffusion and shear on micro-
462 scale nutrient patches, and implications for bacterial chemotaxis. *Marine Ecology*
463 *Progress Series* 189, 1-7.
- 464 Blackburn, N., Fenchel, T., and Mitchell, J. (1998). Microscale nutrient patches in a
465 planktonic habitats shown by chemotactic bacteria. *Science* 282, 2254-2256.
- 466 Bouvy, M., Combe, M., Bettarel, Y., Dupuy, C., Rochelle-Newall, E., and Charpy, L. (2012).
467 Uncoupled viral and bacterial distributions in coral reef waters of Tuamotu
468 Archipelago (French Polynesia). *Marine Pollution Bulletin* 65, 506-515.
- 469 Brentnall, S.J., Richards, K.J., Brindley, J., and Murphy, E. (2003). Plankton patchiness and
470 its effect on larger-scale productivity. *Journal of Plankton Research* 25, 121-140.

- 471 Brumley, D.R., Carrara, F., Hein, A.M., Yawata, Y., and Levin, S.A. (2019). Bacteria push
472 the limits of chemotactic precision to navigate dynamic chemical gradients. *PNAS*, 1-
473 6.
- 474 Brussaard, C.P.D. (2004). Optimization of procedures for counting viruses by flow cytometry.
475 *Applied and Environmental Microbiology* 70, 1506-1513.
- 476 Calbet, A., and Landry, M. R. (2004). Phytoplankton growth, microzooplankton grazing, and
477 carbon cycling in marine systems. *Limnology and Oceanography*. 49, 51-57.
- 478 Carreira, C., Larsen, M., Glud, R.N., Brussaard, C.P.D., and Middelboe, M. (2013).
479 Heterogeneous distribution of prokaryotes and viruses at the microscale in a tidal
480 sediment. *Aquatic Microbial Ecology* 69, 183-192.
- 481 Carreira, C., Piel, T., Staal, M., Stuut, J.-B.W., Middelboe, M., and Brussaard, C.P.D. (2015).
482 Microscale spatial distributions of microbes and viruses in intertidal photosynthetic
483 microbial mats. *SpringerPlus* 4.
- 484 Cushman-Roisin, B. (2019). *Environmental Fluid Mechanics*. John Wiley & Sons, Inc.
- 485 Datta, M.S., Sliwerska, E., Gore, J., Polz, M.F., and Cordero, O.X. (2015). Microbial
486 interactions lead to rapid micro-scale successions on model marine particles. *Nature*
487 *Communications* 7.
- 488 Dun, O.J. (1964). Multiple Comparisons Using Rank Sums. *Technometrics* 6, 241-261.
- 489 Durham, W.M., Climent, E., Barry, M., De Lillo, F., Boffetta, G., Cencini, M., and Stocker,
490 R. (2013). Turbulence drives microscale patches of motile phytoplankton. *Nature*
491 *communications* 4.
- 492 Fenchel, T. (2002). Microbial behavior in a heterogenous world. *Science* 296, 1068-1071.
- 493 Forterre, P., Soler, N., Krupovic, M., Marguet, E., and Ackermann, H.-W. (2013). Fake virus
494 particles generated by fluorescence microscopy. *Trends in Microbiology* 21, 1-5.

- 495 Furnas, M., Alongi, D., Mckinnon, D., Trott, L., and Skuza, M. (2011). Regional-scale
496 nitrogen and phosphorus budgets for the northern (14°S) and central (17°S) Great
497 Barrier Reef shelf ecosystem. *Continental Shelf Research* 31, 1967-1990.
- 498 Furnas, M., Mitchell, A., Skuza, M., and Brodie, J. (2005). In the other 90%: phytoplankton
499 responses to enhanced nutrient availability in the Great Barrier Reef Lagoon. *Marine*
500 *Pollution Bulletin* 51, 253-265.
- 501 Gasol, J.M., Zweifel, U.L., Peters, F., Fuhrman, J.A., and Hagstrom, Å. (1999). Significance
502 of size and nucleic acid content heterogeneity as measured by flow cytometry in
503 natural planktonic bacteria. *Applied and Environmental Microbiology* 65, 4475-4483.
- 504 Giorgio, P.a.D., and Scarborough, G. (1995). Increase in the proportion of metabolically
505 active bacteria along gradients of enrichment in freshwater and marine plankton:
506 implications for estimates of bacterial growth and production rates. *Journal of*
507 *Plankton Research* 17, 1905-1924.
- 508 Hansen, H.P., and Koroleff, F. (1999). "Automated chemical analysis," in *Methods of*
509 *seawater analysis*, eds. K. Grasshoff, K. Kermling & M. Ehrhardt. Wiley-VCH), 159-
510 226.
- 511 Hütz A, S.K., Overmann J (2011). *Thalassospira* sp. isolated from the oligotrophic eastern
512 Mediterranean sea exhibits chemotaxis toward inorganic phosphate during starvation.
513 *Applied Environmental Microbiology* 77, 4412-4421.
- 514 Jickells, T.D., Liss, P.S., Broadgate, W., Turner, S., Kettle, A.J., Read, J., Baker, J., Cardenas,
515 L.M., Carse, F., Hamren-Larssen, M., Spokes, L., Steinke, M., Thompson, A.,
516 Watson, A., Archer, S.D., Bellerby, R.G.J., Law, C.S., Nightingale, P.D., Liddicoat,
517 M.I., Widdicombe, C.E., Bowie, A., Gilpin, L.C., Moncoiffé, G., Savidge, G., Preston,
518 T., Hadziabdic, P., Frost, T., Upstill-Goddard, R., Pedrós-Alió, C., Simó, R., Jackson,

- 519 A., Allen, A., and Degrandpre, M.D. (2008). A Lagrangian biogeochemical study of
520 an eddy in the Northeast Atlantic. *Progress in Oceanography* 76, 366-398.
- 521 Johnson, R.A., and Wichern, D.W. (2007). *Applied multivariate statistical analysis*. Prentice-
522 Hall.
- 523 Kiørboe, T. (2001). Formation and fate of marine snow: small-scale processes with large-
524 scale implications. *Scientia Marina* 65, 57-71.
- 525 Lambrechts, J., Humphrey, C., Mckinna, L., Gourage, O., Fabricius, K.E., Mehta, A.J., Lewis,
526 S., and Wolanski, E. (2010). Importance of wave-induced bed liquefaction in the fine
527 sediment budget of Cleveland Bay, Great Barrier Reef. *Estuarine, Coastal and Shelf*
528 *Science* 89, 154-162.
- 529 Lønborg, C., Álvarez-Salgado, X.A., Duggan, S., and Carreira, C. (2018). Organic matter
530 bioavailability in tropical coastal waters: The Great Barrier Reef. *Limnology &*
531 *Oceanography* 63, 1015-1035.
- 532 Lønborg, C., Doyle, J., Furnas, M., Menendez, P., Benthuisen, J.A., and Carreira, C. (2017).
533 Seasonal organic matter dynamics in the Great Barrier Reef lagoon: Contribution of
534 carbohydrates and proteins. *Continental Shelf Research* 138, 95-105.
- 535 Malmcrona-Friberg, K., Goodman, A., and Kjelleberg, S. (1990). Chemotactic responses of
536 marine *Vibrio* sp. strain S14 (CCUG 15956) to low-molecular-weight substances
537 under starvation and recovery conditions. *Applied and Environmental Microbiology*
538 56, 3699-3704.
- 539 Pinhassi, J., Gómez-Consarnau, L., Alonso-Sáez, L., Sala, M.M., Vidal, M., Pedrós-Alió, C.,
540 and Gasol, J.M. (2006). Seasonal changes in bacterioplankton nutrient limitation and
541 their effects on bacterial community composition in the NW Mediterranean Sea.
542 *Aquatic Microbial Ecology* 44, 241-252.
- 543 Pope, S.B. (2000). *Turbulent Flows*. Cambridge University Press.

- 544 Revelante, N., Williams, W.T., and Bunt, J.S. (1982). Temporal and spatial distribution of
545 diatoms, dinoflagellates and *Trichodesmium* in waters of the Great Barrier Reef.
546 *Journal of Experimental Marine Biology and Ecology* 63, 22-45.
- 547 Seymour, J.R., Patten, N., Bourne, D.G., and Mitchell, J.G. (2005). Spatial dynamics of virus-
548 like particles and heterotrophic bacteria within a shallow coral reef system. *Marine*
549 *Ecology Progress Series* 288, 1-8.
- 550 Seymour, J.R., Seuront, L., Doubell, M., Waters, R.L., and Mitchell, J.G. (2006). Microscale
551 patchiness of virioplankton. *Journal of the Marine Biological Association of the*
552 *United Kingdom* 86, 551-561.
- 553 Stocker, R., and Seymour, J.R. (2012). Ecology and Physics of Bacterial Chemotaxis in the
554 Ocean. *Microbiology and Molecular Biology Reviews* 76, 792-812.
- 555 Stocker, R., Seymour, J.R., Samadani, A., Hunt, D.E., and Polz, M.F. (2008). Rapid
556 chemotactic response enables marine bacteria to exploit ephemeral microscale nutrient
557 patches. *Proceedings of the National Academy of Sciences* 105, 4209-4214.
- 558 Strickland, J.D.H., and Parsons, T.R. (1972). A practical handbook of seawater analysis. *Bull*
559 *Fish Res Board Can* 167, 1-310.
- 560 Suttle, C.A. (2005). Viruses in the sea. *Nature* 437, 356-361.
- 561 Uthicke, S., Furnas, M., and Lønborg, C. (2014). Coral reefs on the edge? Carbon chemistry
562 on inshore reefs of the Great Barrier Reef. *PLoS ONE* 9.
- 563 Wiens, J.A. (1989). Spatial scaling in ecology. *Functional Ecology* 3, 385-397.
- 564 Wigington, C.H., Sonderegger, D., Brussaard, C.P.D., Buchan, A., Finke, J.F., Fuhrman, J.A.,
565 Lennon, J.T., Middelboe, M., Suttle, C.A., Stock, C., Wilson, W.H., Wommack, K.E.,
566 Wilhelm, S.W., and Weitz, J.S. (2016). Re-examination of the relationship between
567 marine virus and microbial cell abundances. *Nature Microbiology*, 1-8.
- 568

Table 1 (on next page)

Sampling sites information

Great Barrier Reef (Australia) location names, sites identification number, latitude, longitude, sampling date, time, and the in-situ salinity and temperature. Sites 1 to 5 were each sampled once for the spatial study, while site 6 was sampled over 4 days for the temporal study.

Location	Site	Latitude	Longitude	Date	Time	Salinity	Temperature (°C)
Rudder Reef	1	-16.20139	145.76722	17/12/2014	8:00 AM	35.5	30.1
Irene Reef	2	-15.64772	145.68234	17/12/2014	2:50 PM	n.d.	n.d.
Osterlund Reef	3	-15.55405	145.45964	18/12/2014	11:00 AM	35.6	29.4
Coral Sea	4	-15.55972	145.97222	19/12/2014	11:20 AM	35.3	28.8
Flora Reef	5	-17.22020	146.25450	22/12/2014	11:00 AM	35.5	28.7
Bowling Green Bay	6	-19.27602	147.05744	12-15/01/2015	High Tide	32 - 33	31 - 32

1

Table 2(on next page)

Spatial study data

Total and per site average (\pm standard deviation, SD), minimum (Min) and maximum (Max) values for nitrate/nitrite ($\text{NO}_3^-/\text{NO}_2^-$), phosphate (HPO_4^{2-}), dissolved organic carbon (DOC), total dissolved nitrogen (TDN), chlorophyll *a* (chl *a*), bacterial and viral abundances, and virus to bacteria ratio (VBR) measured at the sites 1 to 5 included in the spatial study in the Great Barrier Reef (Australia); n.d. - not determined.

Site	Calculation	NO ₃ /NO ₂ ⁻ (μmol l ⁻¹)	HPO ₄ ²⁻ (μmol l ⁻¹)	DOC (μmol l ⁻¹)	TDN (μmol l ⁻¹)	Chl a (μg l ⁻¹)	Bacteria (x10 ⁵ ml ⁻¹)	Viruses (x10 ⁵ ml ⁻¹)	VBR
1	Average ± SD	0.07 ± 0.02	0.06 ± 0.02	90 ± 9	8.4 ± 0.9	0.44 ± 0.21	7.8 ± 0.5	51.9 ± 3.4	6.7 ± 0.7
	Min - Max	0.06 - 0.05	0.04 - 0.09	75 - 106	6.9 - 10.2	0.11 - 0.88	7.3 - 9.6	45.6 - 60.6	3.5 - 7.4
	CV (%)	37	27	10	11	47	7	6	10
2	Average ± SD	0.06 ± 0.01		83 ± 11	6.5 ± 0.8	0.50 ± 0.21	9.6 ± 0.3	58.2 ± 8.8	6.1 ± 1.0
	Min - Max	0.05 - 0.08	n.d.	72 - 112	5.3 - 8.6	0.14 - 0.79	8.8 - 10.2	35.6 - 72.8	3.5 - 7.4
	CV (%)	20		13	12	43	4	15	16
3	Average ± SD	0.08 ± 0.01	0.05 ± 0.01	85 ± 11	6.8 ± 1.6	0.51 ± 0.23	12.5 ± 1.9	47.0 ± 6.9	3.8 ± 0.6
	Min - Max	0.05 - 0.10	0.04 - 0.07	72 - 112	2.1 - 10.1	0.06 - 1.12	11.2 - 20.5	37.7 - 67.2	2.8 - 4.7
	CV (%)	15	21	13	24	46	15	15	15
4	Average ± SD	0.06 ± 0.01	0.07 ± 0.01	89 ± 8	6.5 ± 0.6	0.34 ± 0.18	5.5 ± 0.3	18.9 ± 1.1	3.4 ± 0.3
	Min - Max	0.05 - 0.11	0.04 - 0.11	77 - 104	5.6 - 7.7	0.04 - 0.69	5.2 - 6.5	17.4 - 21.4	2.9 - 4.1
	CV (%)	21	20	9	9	54	5	6	9
5	Average ± SD	0.05 ± 0.01	0.04 ± 0.01	86 ± 5	8.1 ± 1.1	0.25 ± 0.17	10.1 ± 0.6	41.3 ± 2.7	4.1 ± 0.3
	Min - Max	0.05 - 0.07	0.04 - 0.08	78 - 102	6.1 - 10.4	0.05 - 0.62	9.4 - 12.5	36.2 - 45.3	3.2 - 4.7
	CV (%)	10	20	6	13	68	6	7	9
Total	Average ± SD	0.06 ± 0.02	0.06 ± 0.02	86 ± 9	7.3 ± 1.3	0.41 ± 0.22	9.1 ± 2.5	43.4 ± 14.5	4.8 ± 1.5
	Min - Max	0.05 - 0.16	0.04 - 0.11	72 - 112	2.1 - 10.4	0.04 - 1.12	5.2 - 20.5	17.4 - 72.8	2.8 - 8.3

Table 3(on next page)

Temporal study data

Total and per day average (\pm standard deviation, SD), and minimum (Min) and maximum (Max) values for nitrate/nitrite ($\text{NO}_3^-/\text{NO}_2^-$), phosphate (HPO_4^{2-}), dissolved organic carbon (DOC), total dissolved nitrogen (TDN), chlorophyll *a* (chl *a*), bacterial and viral abundances, and virus to bacteria ratio (VBR) measured during the 4 days of the temporal study at Bowling Green Bay (site 6) in the Great Barrier Reef (Australia); n.d. - not determined.

Day	Calculation	NO ₃ ⁻ /NO ₂ ⁻ (μmol l ⁻¹)	HPO ₄ ²⁻ (μmol l ⁻¹)	DOC (μmol l ⁻¹)	TDN (μmol l ⁻¹)	Chl a (μg l ⁻¹)	Bacteria (x10 ⁵ ml ⁻¹)	Viruses (x10 ⁵ ml ⁻¹)	VBR
1	Average ± SD	0.06 ± 0.03	0.08 ± 0.01	107 ± 4	8.9 ± 0.8	0.27 ± 0.18	20.3 ± 0.9	98.9 ± 9.2	4.9 ± 0.5
	Min - Max	0.05 - 0.18	0.06 - 0.09	99 - 114	7.2 - 10.5	0.02 - 0.67	18.8 - 23.0	81.6 - 126.0	4.0 - 6.4
	CV (%)	45	12	4	9	65	5	9	10
2	Average ± SD	0.08 ± 0.0	0.07 ± 0.01	101 ± 4		0.24 ± 0.15	19.8 ± 2.0	121.1 ± 15.7	6.2 ± 1.0
	Min - Max	0.05 - 0.11	0.05 - 0.09	95 - 110	n.d.	0.01 - 0.63	17.8 - 25.3	90.2 - 155.0	4.4 - 8.4
	CV (%)	19	13	4		63	10	13	16
3	Average ± SD	0.18 ± 0.02	0.09 ± 0.01	118 ± 6		0.16 ± 0.12	17.9 ± 3.3	111.0 ± 12.4	6.4 ± 1.3
	Min - Max	0.15 - 0.21	0.07 - 0.11	109 - 135	n.d.	0.05 - 0.67	13.0 - 24.1	94.8 - 160.0	4.0 - 8.2
	CV (%)	10	10	5		76	19	11	20
4	Average ± SD	0.63 ± 0.09	0.11 ± 0.03	100 ± 4	11.3 ± 0.7	0.20 ± 0.10	14.5 ± 0.9	88.1 ± 10.6	6.1 ± 0.7
	Min - Max	0.47 - 0.82	0.07 - 0.16	94 - 113	10.2 - 12.7	0.07 - 0.48	12.1 - 16.4	68.8 - 108.0	5.0 - 7.3
	CV (%)	15	26	4	6	52	6	12	12
Total	Average ± SD	0.24 ± 0.24	0.09 ± 0.02	106 ± 8	10.1 ± 1.4	0.22 ± 0.14	18.1 ± 3.1	104.8 ± 17.3	5.9 ± 1.1
	Min - Max	0.05 - 0.82	0.05 - 0.16	94 - 135	7.2 - 12.7	0.01 - 0.67	12.1 - 25.3	68.8 - 160.0	4.0 - 8.4

Figure 1

Sampling locations

Map showing the sampled location for study sites along the Great Barrier Reef (Australia).
Larger map is a representation of the square indicated in the smaller map of Australia.

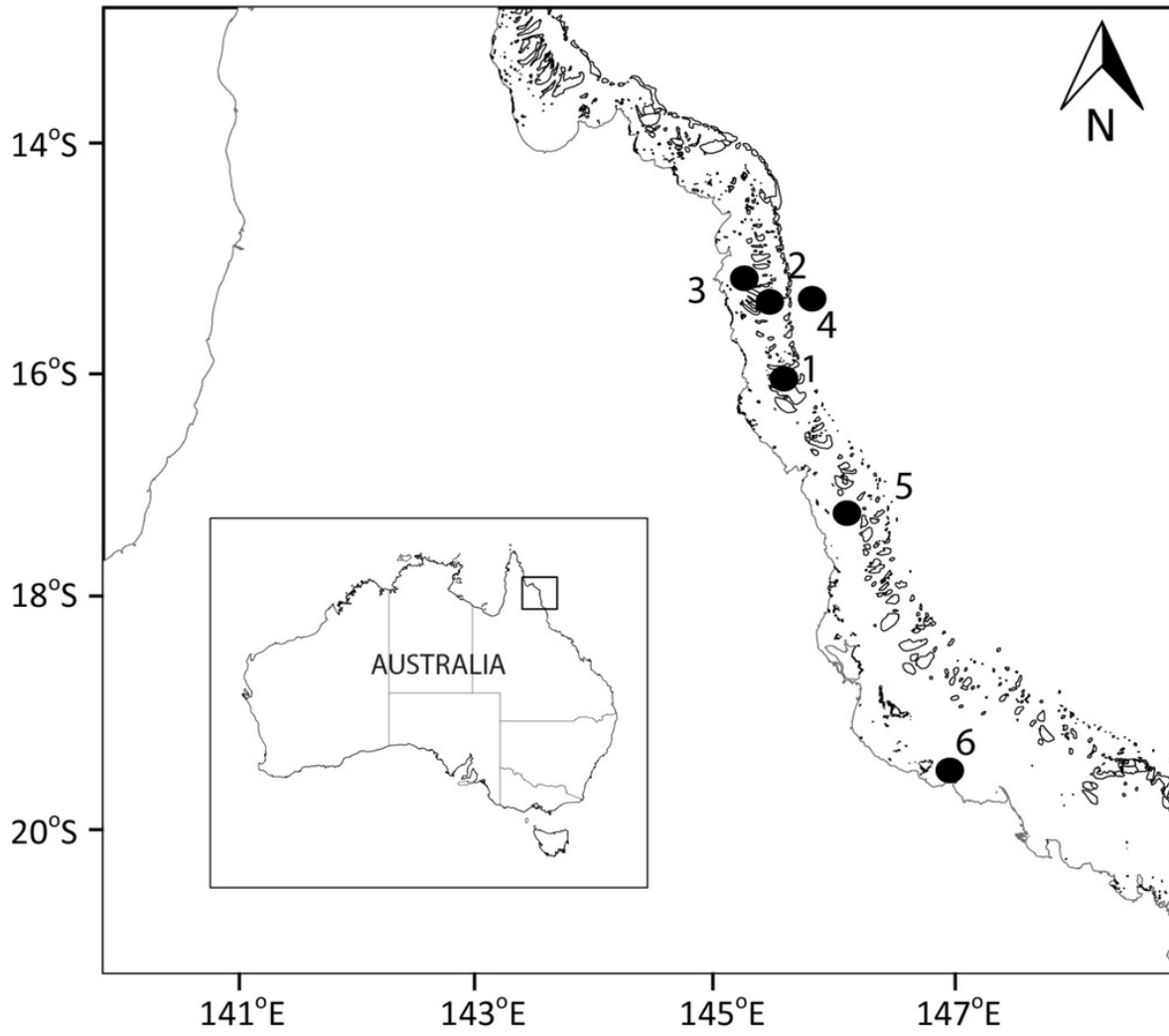


Figure 2

Sampling device

Two-dimensional device used for sampling consisting of 25 inlets (5 x 5) connected to a 25 mL syringe, each separated by 7 cm with a total sampling area of 784 cm².



Figure 3

Spatial distribution of chemical parameters

Small-scale spatial distribution of nitrate/nitrite ($\text{NO}_3^-/\text{NO}_2^-$), phosphate (HPO_4^{2-}), dissolved organic carbon (DOC), total dissolved nitrogen (TDN; top to bottom) measured at the 5 sites (left to right) of the spatial study in the Great Barrier Reef (Australia). The grey scale represents the range of concentrations for each parameter, with white being the lowest concentration and black the highest. The axes represent the 28 cm spatial array used for sampling.

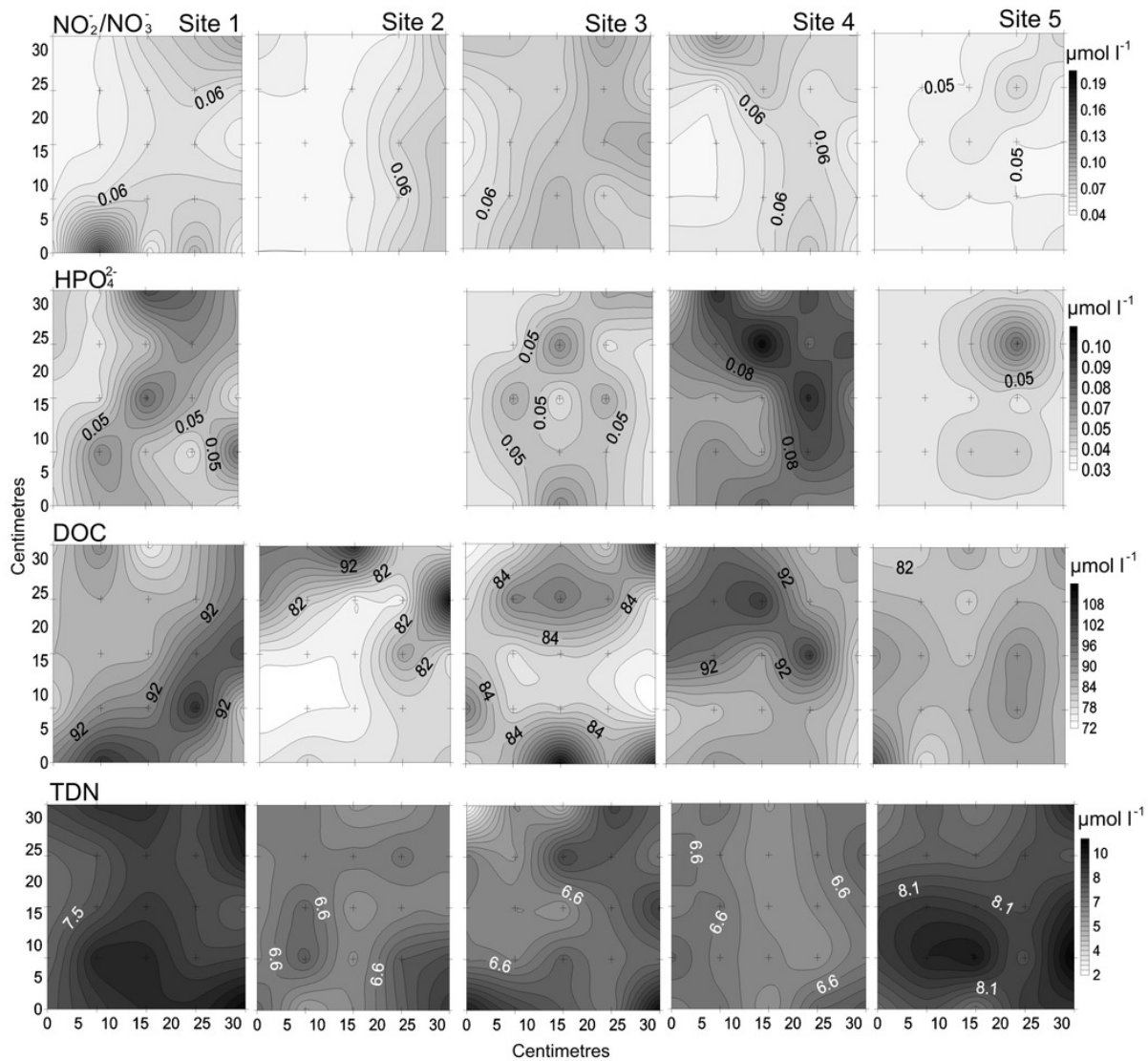


Figure 4

Spatial distribution of biological parameters

Small-scale spatial distribution of chlorophyll *a* (chl *a*), bacteria, viruses, and virus-to bacteria ratio (VBR; top to bottom) measured at the 5 sites (left to right) of the spatial study in the Great Barrier Reef (Australia). The grey scale represents the range of concentrations for each parameter, with white being the lowest concentration and black the highest. The axes represent the 28 cm spatial array used for sampling.

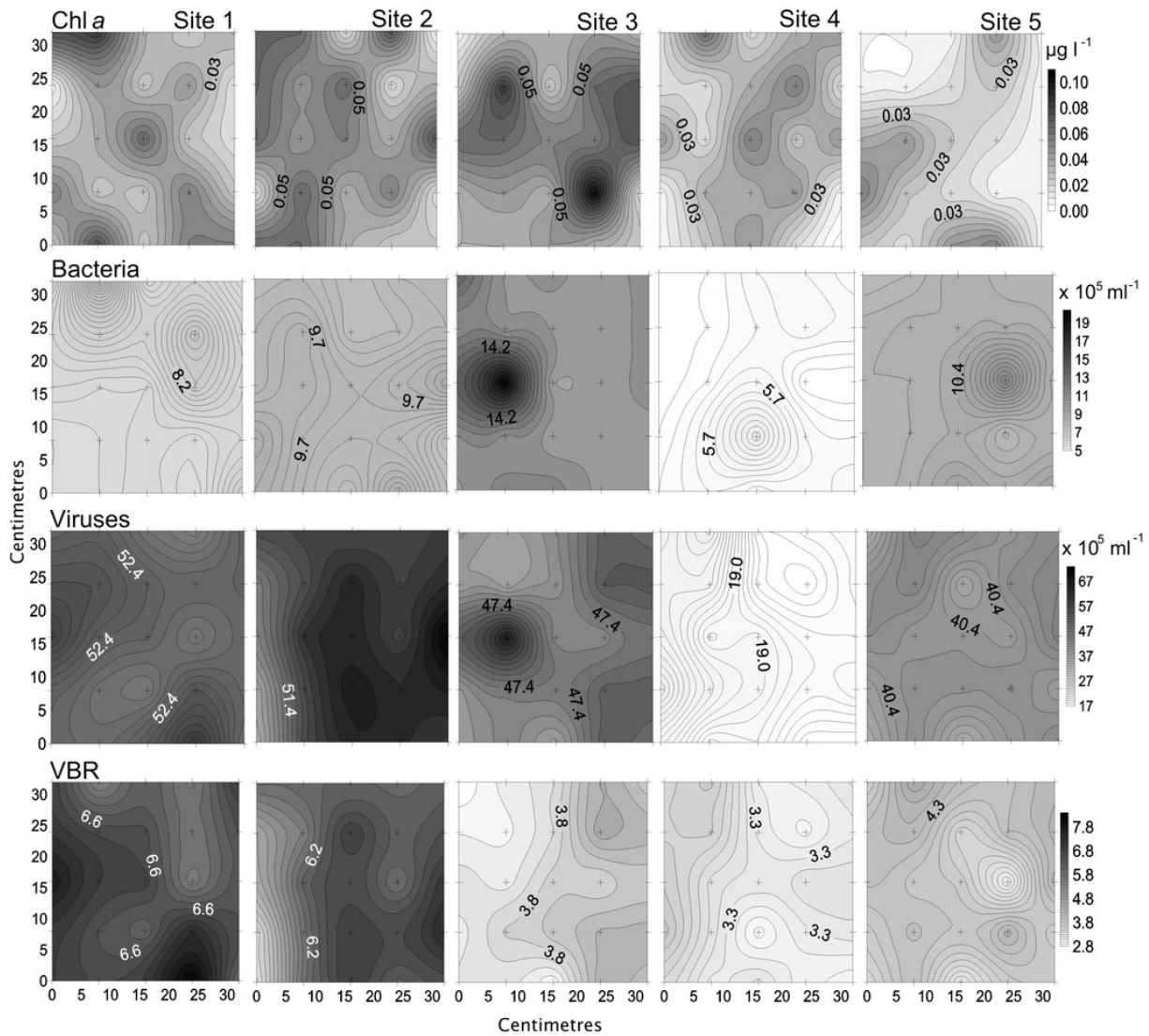


Figure 5

Temporal distribution of chemical parameters

Small-scale spatial distribution of nitrate/nitrite ($\text{NO}_3^-/\text{NO}_2^-$), phosphate (HPO_4^{2-}), dissolved organic carbon (DOC), total dissolved nitrogen (TDN; top to bottom) measured during the 4 days (left to right) of the temporal study in the Great Barrier Reef (Australia). The grey scale represents the range of concentrations for each parameter, with white being the lowest concentration and black the highest. The axes represent the 28 cm spatial array used for sampling.

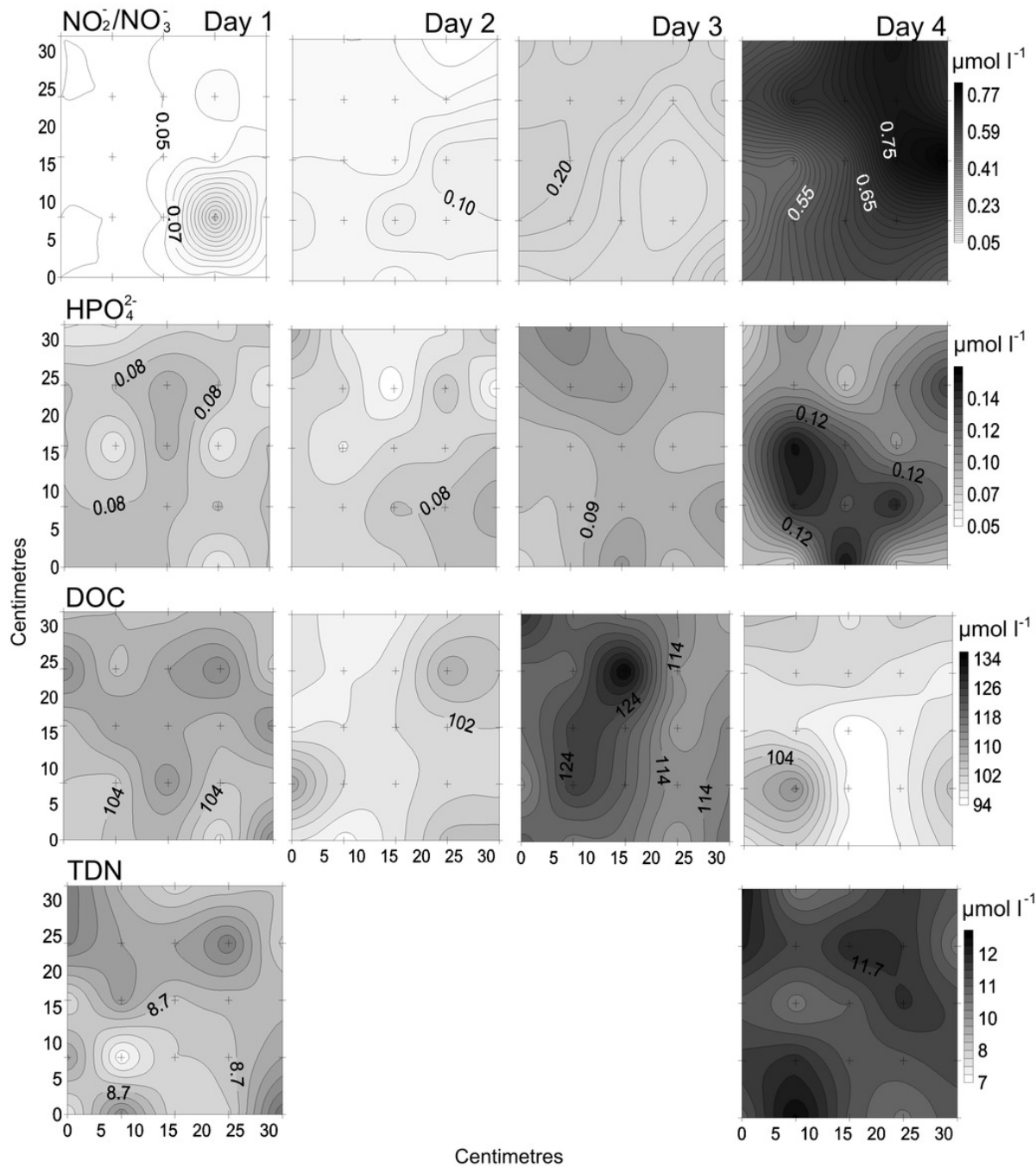


Figure 6

Temporal distribution of biological parameters

Small-scale spatial distribution of chlorophyll *a* (chl *a*), bacteria, viruses, and the virus to bacteria ratio (VBR; top to bottom) measured during the 4 days (left to right) of the temporal study in the Great Barrier Reef (Australia). The grey scale represents the range of concentrations for each parameter, with white being the lowest concentration and black the highest. The axes represent the 28 cm spatial array used for sampling.

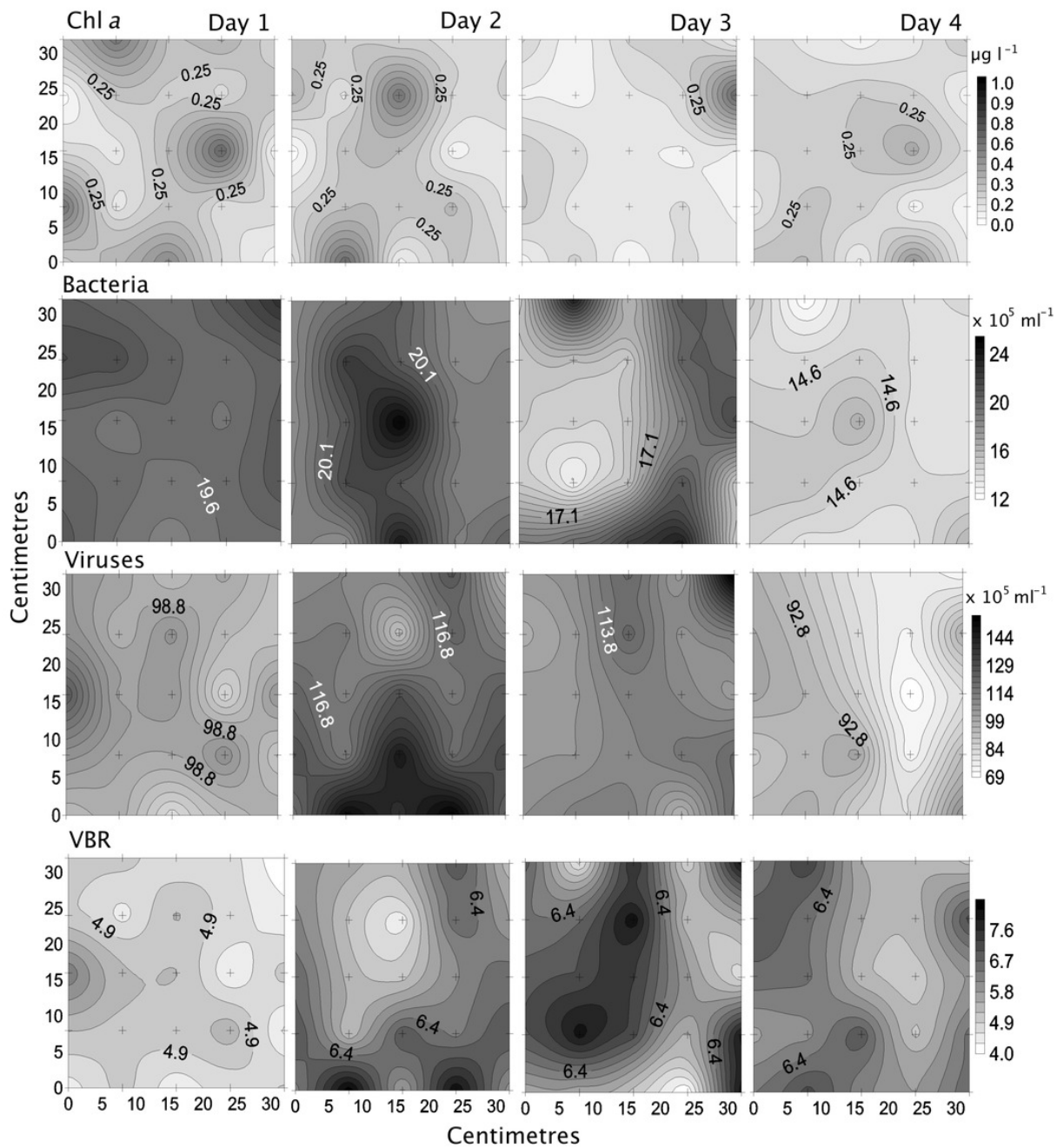


Figure 7

Spatial distribution of biological parameters at large-scale

Boxplots of each chemical (A-nitrate/nitrite - $\text{NO}_3^-/\text{NO}_2^-$, B-phosphate - HPO_4^{2-} , C-dissolved organic carbon - DOC, and D-total dissolved nitrogen - TDN), and biological parameter (E-chlorophyll *a* - chl *a*, F-bacteria, and G-viruses) for the sampled sites (1, 2, 3, 4, and 5) in the Great Barrier Reef (Australia). Error bars represent the 10th and 90th percentiles, with 50 % of the data inside the box. The solid line inside the box represents the median. Each site had a sample size of $n = 25$. Boxplots showing the same letter are not significantly different ($P < 0.05$).

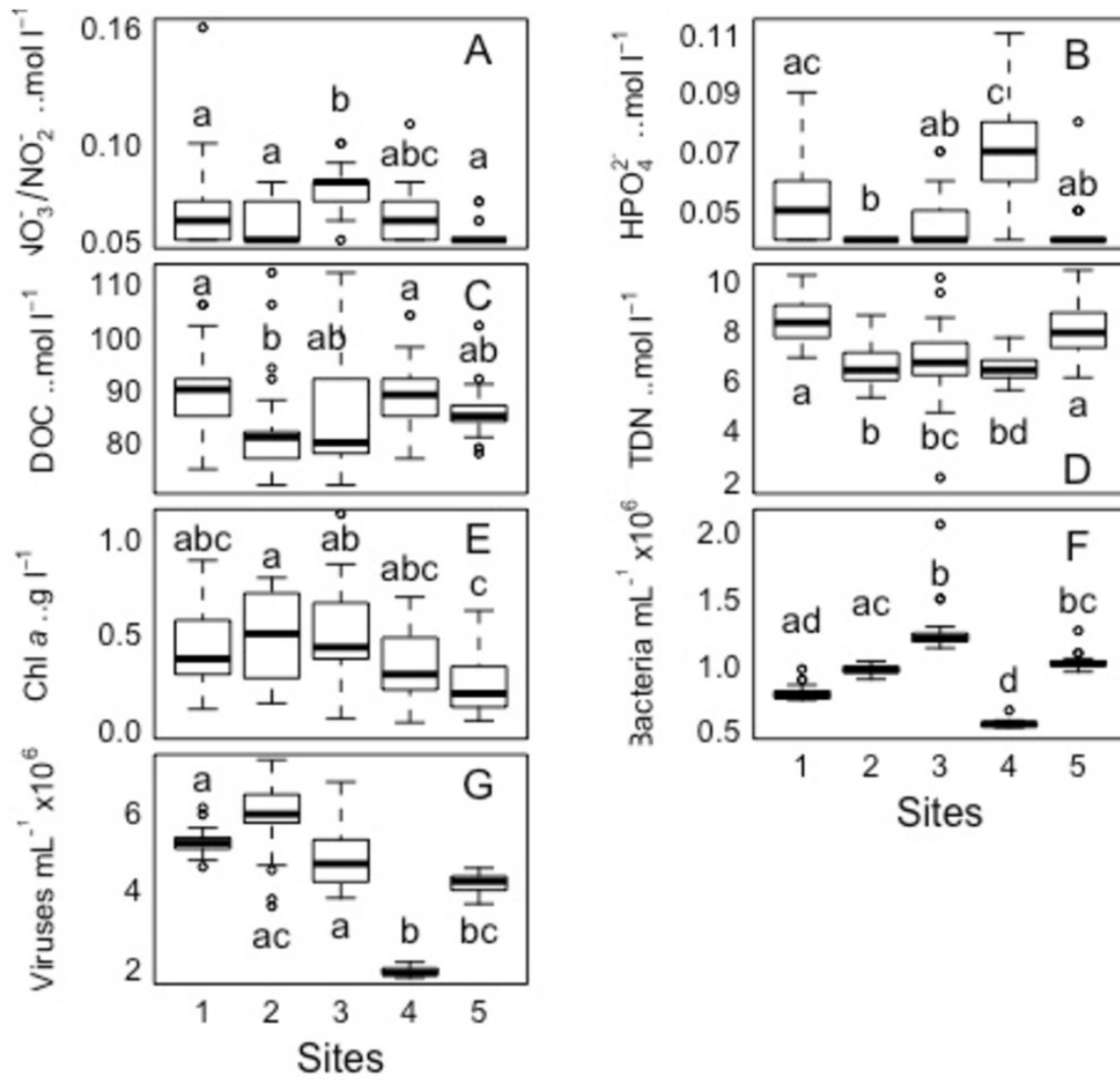


Figure 8

Temporal distribution of biological parameters at large-scale

Boxplots of each chemical (A-nitrate/nitrite - $\text{NO}_3^-/\text{NO}_2^-$, B-phosphate - HPO_4^{2-} , and C-dissolved organic carbon - DOC), and biological parameter (D-chlorophyll *a* - chl *a*, E-bacteria, and F-viruses) for the sampled days (1, 2, 3, and 4) in the Great Barrier Reef (Australia) at Bowling Green Bay (site 6). Error bars represent the 10th and 90th percentiles, with 50 % of the data inside the box. The solid line inside the box represents the median. Each day had a sample size of $n = 25$. Boxplots showing the same letter are not significantly different ($P < 0.05$).

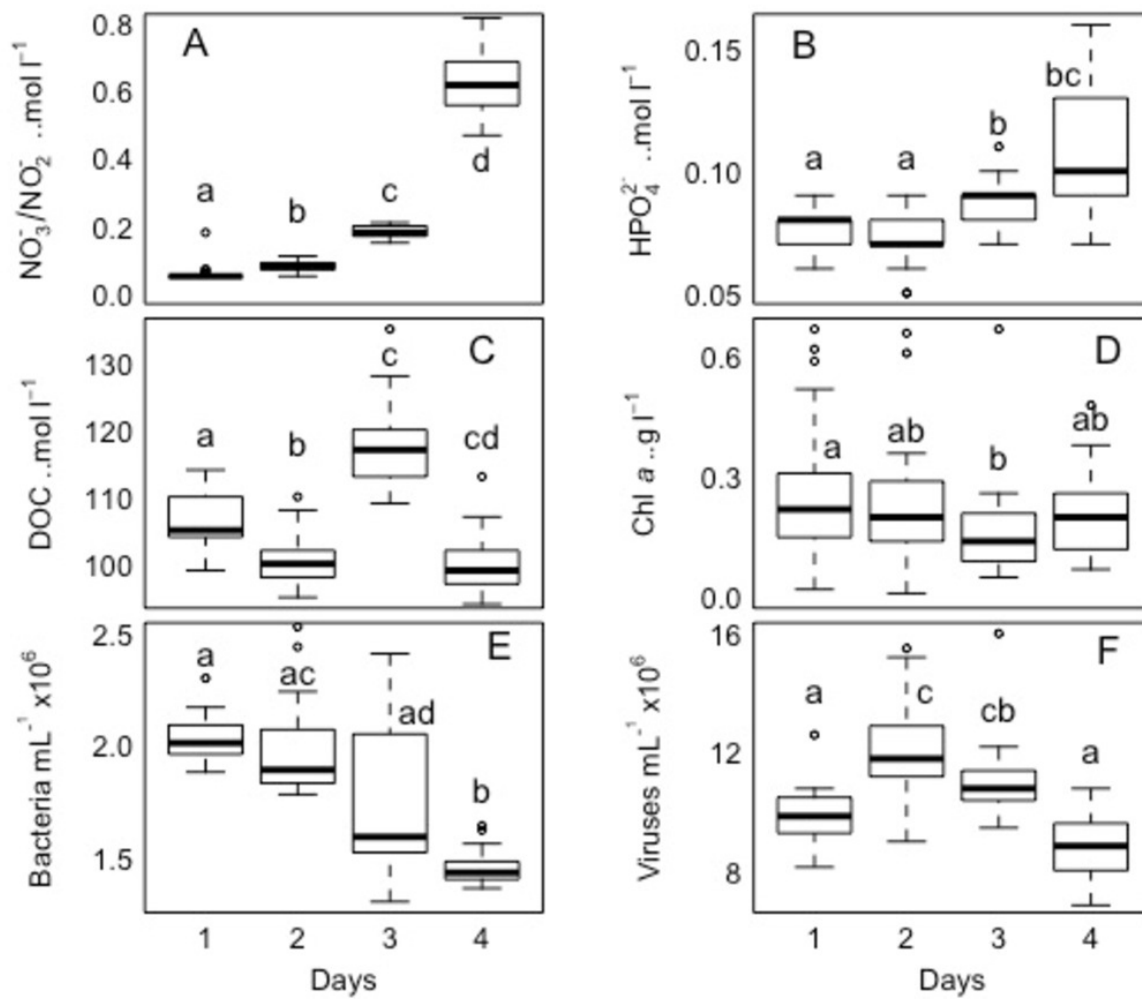


Figure 9

Linear regression

Between the abundances of bacteria and viruses from all the sites (1, 2, 3, 4, and 5) and days (1,2, 3, and 4) measured in the Great Barrier Reef (Australia) ($n = 325$; $R^2 = 0.75$; $p < 0.0001$; $\text{Vir} = 5.4 \pm 0.3 \text{ Bact}$).

